

Optimal Control of Behavioral-Feedback SIR Epidemic Model

Martina Alutto, *Member, IEEE*, Leonardo Cianfanelli, *Member, IEEE*, Giacomo Como, *Member, IEEE*, Fabio Fagnani *Member, IEEE*, and Francesca Parise *Member, IEEE*

Abstract—We consider a behavioral-feedback SIR epidemic model, in which the infection rate depends in feedback on the fractions of susceptible and infected agents, respectively. The considered model allows one to account for endogenous adaptation mechanisms of the agents in response to the epidemics, such as voluntary social distancing, or the adoption of face masks. For this model, we formulate an optimal control problem for a social planner that has the ability to reduce the infection rate to keep the infection curve below a certain threshold within an infinite time horizon, while minimizing the intervention cost. Based on the dynamic properties of the model, we prove that, under quite general conditions on the infection rate, the *filling the box* strategy is the optimal control. This strategy consists in letting the epidemics spread without intervention until the threshold is reached, then applying the minimum control that leaves the fraction of infected individuals constantly at the threshold until the reproduction number becomes less than one and the infection naturally fades out. Our result generalizes one available in the literature for the equivalent problem formulated for the classical SIR model, which can be recovered as a special case of our model when the infection rate is constant. Our contribution enhances the understanding of epidemic management with adaptive human behavior, offering insights for robust containment strategies.

Index Terms—Epidemic models, Susceptible-Infected-Recovered model, Optimal control problem.

I. INTRODUCTION

The spread of infectious diseases has always been a serious threat to public health. To reduce their impact, it is essential to design effective containment strategies. However, this task is challenging because it requires taking into account several factors, such as the capacity of the healthcare system and the social and economic consequences of interventions. When

the resources are limited, it becomes especially important to identify policies that use them in the most effective way.

In recent years, mathematical models have become important tools for predicting how outbreaks evolve and for assessing the effectiveness of different control strategies. Deterministic compartmental models play a central role in capturing the essential features of disease transmission and supporting the formulation of public health strategies. Among these, the Susceptible-Infected-Recovered (SIR) model is one of the most extensively studied because of its simplicity and generality [2]–[5]. It divides the population into three compartments (susceptible, infected, and recovered) and describes their evolution in time through a system of nonlinear differential equations, assuming that the population is large, homogeneous, and well mixed.

However, a key limitation of the classical SIR model is its assumption of a constant infection rate, disregarding behavioral adaptations. Historical and recent evidence shows that agents change their behavior in response to perceived infection risk, affecting contact patterns and, consequently, the disease transmission. For example, during the 1918 influenza pandemic people avoided crowded areas [6], during the SARS outbreak, widespread use of face masks and reduced travel were observed [7], and during the recent COVID-19 pandemic behavioral responses were further reinforced by government measures such as social distancing and lockdowns [8].

To incorporate the human behavior into epidemic models, two main approaches have emerged. The first one consists in adding to the system new dynamic variables, often based on *evolutionary game theory* [9], to model how the agents weigh the costs and benefits of actions like vaccination or isolation based on their risk perception and on social influence. The infection rate is then assumed to depend on such variables, which in turn depend on the epidemic state [10]–[17]. The drawback of this approach is that the number of variables of the system increases, making optimal control problems often analytically intractable.

The second main modeling approach incorporates the human behavior through static feedback mechanisms. In these *behavioral-feedback SIR epidemic models*, the infection rate β is a function of the current epidemic state rather than dependent on additional dynamic variables or constant as in the classical SIR model [18], [19]. A seminal contribution for this class of models is [20], which introduced a SIR model where the infection rate β decreases with the fraction of infected agents y , producing a unimodal infection curve. Later

Martina Alutto, Leonardo Cianfanelli, Giacomo Como and Fabio Fagnani are with the Department of Mathematical Sciences “G.L. Lagrange,” Politecnico di Torino, 10129 Torino, Italy. E-mail: {martina.alutto;leonardo.cianfanelli;giacomo.como;fabio.fagnani}@polito.it. Martina Alutto is also with the Institute of Electronics, Computer and Telecommunication Engineering, National Research Council of Italy, Politecnico di Torino, 10129 Torino, Italy. Giacomo Como is also with the Department of Automatic Control, Lund University, 22100 Lund, Sweden. Francesca Parise is with the School of Electrical and Computer Engineering, Cornell University, Ithaca, NY 14850 USA. E-mail: fp264@cornell.edu.

This work was partially supported by the Research Project PRIN 2022 “Extracting Essential Information and Dynamics from Complex Networks” (Grant Agreement number 2022MBC2EZ) funded by the Italian Ministry of University and Research.

This work is based in part on material appearing in the first author’s PhD dissertation [1].

studies confirmed that such feedback can flatten the curve and preserve key stability properties [21]–[23], and that the unimodality of the infection curve is preserved even if the infection rate depends on both the fraction of susceptible agents x and infected agents y [24]. Recent work further explored these effects, deriving bounds on epidemic overshoot and identifying invariants of motion [25], or studying complex nonlinear feedback with saturation effects [26]. Other behavioral-feedback SIR models with non-linear infection rate $\beta(x, y)$ are considered in [27]–[29]. Time-dependent infection rates have also been introduced to reflect seasonal or delayed responses [30].

In this paper, we address an optimal control problem for a class of behavioral-feedback SIR models where the infection rate depends on both the fraction of susceptible agents x and infected agents y . Optimal control of the classical SIR epidemic model has been extensively studied in recent years [31]–[35], particularly for calibrating lockdowns to achieve epidemic control without excessively harming the economy. For example, [36] proposes an optimal control problem for the SIR model over a finite time horizon, where the epidemic cost is linear in the fraction of infected agents, and the economic cost is linear in the level of intervention, proving that the optimal control is bang-bang with at most two switches. In [37], the authors study an optimal control problem where the economic cost depends on both the severity and duration of the lockdown, and the epidemic cost is quadratic in the fraction of infected agents to account for hospital congestion. They prove that, for an infinite time horizon, a strategy that stabilizes the fraction of infected agents outperforms one that stabilizes the reproduction number. Similarly, in [38], the authors solve an optimal control problem numerically for network SIR dynamics, showing that optimal policies differentially targeting risk or age groups significantly outperform uniform policies. In [39] the authors provide the solution of an optimal control problem of the SIR model with infinite time horizon, where an external controller aims to minimize the cost of the intervention while ensuring that the fraction of infected agents remains below a specified threshold at every time. This threshold represents the healthcare system's capacity, referred to as the ICU capacity constraint, ensuring comprehensive care for infected patients. Such constraints reflect scenarios like those observed during COVID-19, where the number of critically ill patients risked exceeding available resources, potentially leading to adverse outcomes. Respecting the ICU constraint guarantees that all patients receive necessary medical care. The optimal strategy consists in setting the minimum lockdown level needed to satisfy the constraint, known as the *filling the box strategy*. In the first stages, the disease spreads uncontrolled, followed by an abrupt lockdown when the infection curves meets the threshold, and then a gradual reopening until a time after which the spread is no longer regulated and the infection naturally fades out. The economic rationale behind this optimal policy is to avoid shutting down society while ICU resources remain unused. Therefore, whenever the natural spread does not threaten the ICU constraint, it should proceed without intervention. This policy is proven to be optimal also in [40], where the authors

propose an optimal control problem for epidemic mitigation that incorporates both molecular and serology testing.

Our main contribution is to prove that, under some mild assumptions on the regularity and monotonicity of feedback mechanism that regulates the infection rate, the filling-the-box strategy is the optimal control for a general class of behavioral-feedback SIR models. This result extends the findings of [39], which apply to the standard SIR model. The proof relies on the properties of the behavioral-feedback SIR model, in particular the unimodality of the infection curve, which is guaranteed under very general assumptions on the feedback mechanism. Compared to [39], the main technical challenge of our analysis is that the class of behavioral feedback SIR models considered in this paper does not admit in general an invariant of motion, which was exploited in [39] to prove the optimality of the filling-the-box strategy.

To the best of our knowledge, this is the first study that jointly addresses the human adaptive behavior and the optimal control of epidemics besides our preliminary results in [41], where the authors study a behavioral-feedback SIR model with a special feedback mechanism, showing that it admits a non-trivial invariant of motion and characterize the infection peak. In addition, [41] analyzes the system under a threshold constraint on the infection level, showing that a feasible control strategy consists in applying the minimal amount of restrictions required to keep the epidemic below a threshold, and they provide an explicit characterization of the associated cost. The main novelties of this work with respect to [41] are the following. First, we consider a general class of feedback mechanisms, rather than focusing on a specific functional form. Within this generalized framework, we prove that under mild conditions on the transmission rate the infection curve remains unimodal, and we rigorously formulate the associated optimal control problem. In this setting, we establish that the filling-the-box strategy is the optimal solution, thus extending the preliminary results of [41] to a much broader class of models, where the analysis cannot rely on invariants of motion and requires different arguments. Finally, we provide a numerical counterexample showing that, when the monotonicity assumptions on the infection rate are relaxed, the filling-the-box strategy is no longer optimal.

The rest of the paper is organized as follows. In Section II we introduce the controlled behavioral-feedback SIR epidemic model, formulate the optimal control problem we aim to study, and present our main result. In Section III, we analyze the uncontrolled dynamics, which is instrumental for the proof of our main result. The proof itself is then provided in Section IV. In Section V, we discuss a counterexample, while in Section VI we summarize our contribution and discuss future research lines.

A. Notation

We briefly gather here some notational conventions adopted throughout the paper. We denote by \mathbb{R} and \mathbb{R}_+ the sets of real and nonnegative real numbers, respectively. We will often consider differentiable functions $f(x, y)$ and use the notation $\dot{f} = f_x \dot{x} + f_y \dot{y}$ to denote the time derivative of the composed

function $f(x(t), y(t))$. Throughout this paper, given an interval $\mathcal{I} \subseteq \mathbb{R}$, we say that $u : \mathcal{I} \rightarrow \mathbb{R}^n$ is a piecewise-continuous function if there exists a subset $\mathcal{W} \subseteq \mathcal{I}$ that does not contain accumulation points and is such that:

- u is continuous on $\mathcal{I} \setminus \mathcal{W}$;
- in every t_0 in \mathcal{W} , u has a jump discontinuity, i.e., the left and right limits

$$u(t_0^-) = \lim_{t \rightarrow t_0^-} u(t), \quad u(t_0^+) = \lim_{t \rightarrow t_0^+} u(t),$$

exist and are finite.

A function $u : \mathcal{I} \rightarrow \mathbb{R}^n$ is a right-continuous if it is piecewise-continuous and $u(t_0) = u(t_0^+)$ for every discontinuity point t_0 . Furthermore, we say that a continuous function $u : \mathcal{I} \rightarrow \mathbb{R}$ is piecewise- \mathcal{C}^1 if, except for a subset \mathcal{W} as above, it is differentiable and u' is piecewise-continuous.

II. CONTROLLED BEHAVIORAL-FEEDBACK SIR EPIDEMIC MODEL

In this section, we introduce the epidemic model studied in this paper and provide our main result.

A. Model Definition

We build our analysis on an epidemic model that describes the spread of a disease within a homogeneous population of agents, incorporating an endogenous feedback mechanism and an exogenous control signal. Before introducing the model, we define the simplex Δ and the space \mathcal{S} by

$$\Delta = \{(x, y, z) \in \mathbb{R}_+^3 : x + y + z = 1\},$$

and

$$\mathcal{S} = \{(x, y) \in \mathbb{R}_+^2 : x + y \leq 1\},$$

respectively. The *controlled behavioral-feedback SIR epidemic model* (CBF-SIR) is the system of ODEs

$$\begin{cases} \dot{x} = -(1-u)\beta(x, y)xy, \\ \dot{y} = (1-u)\beta(x, y)xy - \gamma y, \\ \dot{z} = \gamma y, \end{cases} \quad (1)$$

where

- $x = x(t)$, $y = y(t)$ and $z = z(t)$ indicate the fraction of susceptible, infected and recovered agents, respectively, for every time $t \geq 0$;
- $\beta : \mathcal{S} \rightarrow (0, +\infty)$ is the state-dependent infection rate, which captures the endogenous behavioral response to the epidemics, assumed to be a \mathcal{C}^1 function of (x, y) ;
- $u : \mathbb{R}_+ \rightarrow [0, 1]$ is a right-continuous function of time that models a control signal available to an external controller aiming to limit the disease spread by restricting social interactions. The set of available control signals is

$$\mathcal{U} = \{u : [0, +\infty) \rightarrow [0, 1] \text{ right-continuous}\};$$

- $\gamma > 0$ is the recovery rate from the disease.

The following result establishes the well-posedness of the CBF-SIR model (1) in the simplex Δ .

Proposition 1: Given a state-dependent infection rate β of class \mathcal{C}^1 , a control signal u in \mathcal{U} with jumps in $t_1 < t_2 < \dots$,

and an initial state (x_0, y_0, z_0) in Δ , there exists a unique piecewise- \mathcal{C}^1 function $(x, y, z) : [0, +\infty) \rightarrow \Delta$ that solves the ODE (1) outside the time instants $t_1 < t_2 < \dots$, and is such that

$$x(0) = x_0, \quad y(0) = y_0, \quad z(0) = z_0. \quad (2)$$

Moreover:

- (i) $t \rightarrow x(t)$ is non-increasing for every $t \geq 0$ and is strictly decreasing for every $t \geq 0$ if and only if $x_0 > 0$ and $y_0 > 0$;
- (ii) $y(t) > 0$ for every $t \geq 0$ if and only if $y_0 > 0$;
- (iii) the set of equilibrium points in Δ is

$$\Delta_e = \{(x_e, 0, 1 - x_e) : x_e \in [0, 1]\};$$

- (iv) $(x(t), y(t), z(t))$ converges, for $t \rightarrow +\infty$, to an equilibrium point in Δ_e .

Proof: See Appendix. ■

From now on, we will refer to the vector functions constructed in the previous proposition as to *solutions* of system (1).

Observe that the map $s : \mathcal{S} \rightarrow \Delta$ defined by

$$s(x, y) = (x, y, 1 - x - y),$$

is a bijection from \mathcal{S} to Δ , hence for every time t we can denote the state by the pair $(x(t), y(t))$ in \mathcal{S} and omit $z(t)$, under the implicit assumption that $z(t) = 1 - x(t) - y(t)$. In light of this observation, from now on, we can limit our analysis to the first two equations in (1). After defining the *reproduction number*

$$R(x, y) = \frac{1}{\gamma} \beta(x, y)x, \quad (3)$$

the two equations can be written as

$$\begin{cases} \dot{x} = -(1-u)\gamma R(x, y)y, \\ \dot{y} = \gamma((1-u)R(x, y) - 1)y. \end{cases} \quad (4)$$

From now on we will work with the system of ODEs (4) and refer to it as to the CBF-SIR epidemic model.

To prove both the unimodality of the infection curve and to further show the optimality of the proposed control strategy, we rely on the following standing assumption on the feedback mechanism regulating the infection rate.

Assumption 1: The state-dependent infection rate β satisfies

$$x\beta_x(x, y) + \beta(x, y) > 0, \quad (5)$$

$$\beta_y(x, y) \leq 0, \quad (6)$$

for every (x, y) in \mathcal{S} .

Remark 1: Note that (5)-(6) are equivalent to assuming that the reproduction number $R(x, y)$ is increasing in x and non-increasing in y for every (x, y) in \mathcal{S} .

Equation (5) captures how the infection rate varies with the fraction of susceptible agents. This condition is satisfied when $\beta_x(x, y)$ is positive, e.g., when a higher fraction of susceptible leads to a lower perceived risk, encouraging social interactions and riskier behaviors that facilitate the transmission of the disease. Equation (5) can also be satisfied when $\beta_x(x, y)$ is negative but not too large in magnitude. A negative value of $\beta_x(x, y)$ can be interpreted as the effect of pandemic fatigue,

where agents gradually relax self-protective measures as the epidemic progresses. Indeed, by Proposition 1(i), the fraction of susceptible agents x decreases over time, so this condition reflects an increase in the infection rate as time progresses. Equation (6) captures the tendency of the agents to reduce their interaction level in response to the number of active cases. We remark that (5) generalizes the assumption made in [24], while (6) is a standard assumption in the literature of feedback SIR epidemic models [21], [22].

Example 1: Let $a \geq 0$ and $b : \mathbb{R} \rightarrow (0, +\infty)$ be an arbitrary non-decreasing \mathcal{C}^1 function. The two families of infection rates

$$\beta(x, y) = \frac{b(x)}{1 + ay}, \quad (7)$$

$$\beta(x, y) = b(x)(1 - ay), \quad (8)$$

satisfy (5)-(6). The CBF-SIR epidemic model with infection rate (7) has been studied in [41]. Note that also the classical SIR model may be recovered as a special case from (7)-(8) by letting $a = 0$ and b being a positive constant.

B. Problem Statement

We consider an external controller that designs a control signal u in \mathcal{U} to reduce the infection rate. The goal of the controller is to keep the fraction of infected agents below a threshold \bar{y} in $(0, 1]$, representing for instance the healthcare capacity.

Definition 1: Given \bar{y} in $(0, 1]$ and (x_0, y_0) in \mathcal{S} such that $y_0 \leq \bar{y}$, we say that a control signal u in \mathcal{U} is *feasible* if the solution of the CBF-SIR epidemic model (4) with initial condition (x_0, y_0) satisfies $y(t) \leq \bar{y}$ for every $t \geq 0$. The set of all feasible control signals for a given threshold \bar{y} and initial condition (x_0, y_0) is denoted $\mathcal{U}_{x_0, y_0}^{\bar{y}}$.

Note that $\mathcal{U}_{x_0, y_0}^{\bar{y}}$ is non-empty since it contains the trivial control signal $u \equiv 1$.

The implementation of the control has an associated economic cost that the controller aims to minimize. The cost is modeled by the functional $J : \mathcal{U}_{x_0, y_0}^{\bar{y}} \rightarrow [0, +\infty]$ defined by

$$J(u) = \int_0^{+\infty} u(t) dt.$$

We then consider the optimal control problem

$$V^*(x_0, y_0) = \min_{u \in \mathcal{U}_{x_0, y_0}^{\bar{y}}} J(u). \quad (9)$$

Note that the solution of (9) is trivial if $y_0 = 0$, since Proposition 1(ii) guarantees that in this case $y(t) = 0$ for every $t \geq 0$ under every control signal in \mathcal{U} , including the zero cost control $u \equiv 0$. For this reason, we will work under the assumption that $y_0 > 0$. In the next section we establish our main result, which provides a solution of (9).

C. Main result

We now formulate our main result, whose proof is deferred to Section IV. To this end, let $\mathcal{S}_+ = \{(x, y) \in \mathcal{S} : x > 0, y > 0\}$ and

$$\rho(x, y) = \frac{R(x, y) - 1}{R(x, y)} = 1 - \frac{\gamma}{x\beta(x, y)}, \quad (10)$$

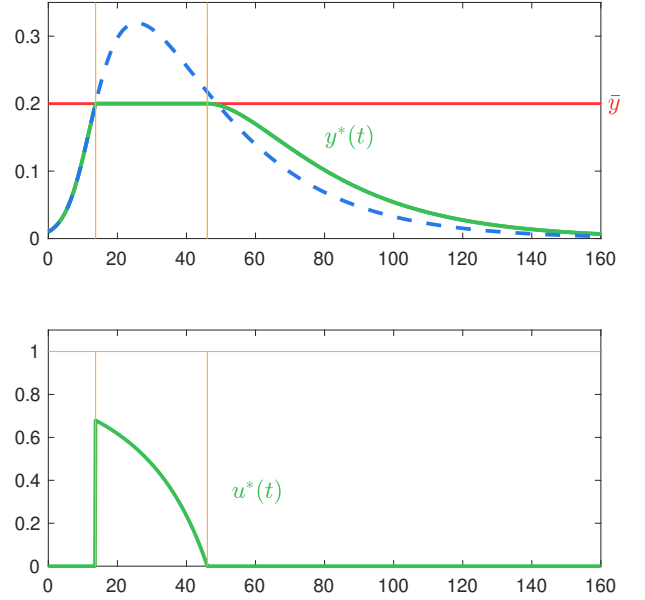


Fig. 1: Numerical simulation of the CBF-SIR epidemic model (4) with $\beta(x, y) = 0.35x(1 - y)$ and $\gamma = 0.05$. The top plot shows in blue the uncontrolled solution and in green the solution corresponding to the optimal control signal $u^*(t)$ (11)-(12) with threshold $\bar{y} = 0.2$. The optimal control signal is reported in the bottom plot.

for every (x, y) in \mathcal{S}_+ .

Theorem 1: Let β be of class \mathcal{C}^2 and let Assumption 1 hold true. Consider a threshold \bar{y} in $(0, 1]$ and an initial condition (x_0, y_0) in \mathcal{S} with $0 < y_0 \leq \bar{y}$. Then, the optimal control problem (9) admits a solution u^* in $\mathcal{U}_{x_0, y_0}^{\bar{y}}$ that has the following feedback representation. Indicating with $(x^*(t), y^*(t))$ the solution of (4) with initial condition (2) under the control signal $u^*(t)$, we have that

$$u^*(t) = \mu(x^*(t), y^*(t)), \quad \forall t \geq 0, \quad (11)$$

where

$$\mu(x, y) = \begin{cases} 0 & \text{if } y < \bar{y} \\ [\rho(x, \bar{y})]_+ & \text{if } y = \bar{y}. \end{cases} \quad (12)$$

Moreover, u^* is unique in $\mathcal{U}_{x_0, y_0}^{\bar{y}}$.

Proof: See Section IV. ■

The optimal feedback policy $u^*(t)$ allows the disease to spread without control until the fraction of infected agents hits the threshold \bar{y} at a certain time T_0 . From there on, the dynamics read

$$\begin{cases} \dot{x}^* = -\gamma\bar{y} \\ \dot{y}^* = 0, \end{cases} \quad (13)$$

hence the fraction of infected remains constantly at the threshold \bar{y} . At time T_1 such that $R(x^*(T_1), \bar{y}) = 1$ (or equivalently, $\rho(x^*(T_1), \bar{y}) = 0$), the control is released, so that the trajectory follows the uncontrolled dynamics and the infection curve

naturally declines from there on. The corresponding control signal $u^*(t)$ starts abruptly above 0 at time T_0 and subsequently is adjusted in time to maintain the fraction of infected exactly at the threshold \bar{y} until T_1 . At that point, the control is deactivated. This policy is known in the literature as *filling-the-box* strategy and its optimality relies on the monotonicity of the reproduction number, which implies the unimodality of the infection curve. Our result generalizes [39], which proved that the filling-the-box strategy is the optimal control of the equivalent optimal control problem formulated for the classical SIR epidemic model, which is a special case of the CBF-SIR epidemic model, as noted in Example 1.

A numerical simulation of the CBF-SIR epidemic model (4) with $\beta(x, y) = 0.35x(1 - y)$, $\gamma = 0.05$, and optimal control signal $u^*(t)$ (11)-(12) with threshold $\bar{y} = 0.2$ is presented in Figure 1. The top plot illustrates in green the solution $y^*(t)$ corresponding to the optimal control signal $u^*(t)$, which is reported in the bottom plot. The dashed blue curve is the corresponding uncontrolled solution, namely, the solution of the CBF-SIR epidemic model (4) with $u \equiv 0$.

The next section analyzes the property of the CBF-SIR epidemic model without control. This analysis will be instrumental for the proof of Theorem 1.

III. UNCONTROLLED BF-SIR EPIDEMIC MODEL

In this section, we analyze the CBF-SIR epidemic model (4) with $u \equiv 0$, i.e., the dynamical system

$$\begin{cases} \dot{x} = -\gamma R(x, y)y, \\ \dot{y} = \gamma[R(x, y) - 1]y. \end{cases} \quad (14)$$

We shall refer to this system of ODE as the (uncontrolled) BF-SIR epidemic model.

A. Unimodality of the infection curve

We start by proving that the infection curve of the uncontrolled BF-SIR epidemic model (14) under condition (5) is unimodal, namely, it admits at most one peak. This result generalizes [24, Theorem 1].

Proposition 2: Consider the uncontrolled BF-SIR epidemic model (14) with initial condition (2) and let (5) hold true. Then:

- (i) if $R(x_0, y_0) \leq 1$, then $t \mapsto y(t)$ is strictly decreasing for $t \geq 0$;
- (ii) if $R(x_0, y_0) > 1$, then there exists a finite time \hat{t} such that $t \mapsto y(t)$ is strictly increasing for t in $[0, \hat{t}]$ and strictly decreasing for $t \geq \hat{t}$;

Proof: It follows from the definition of the reproduction number (3) and from (14) that

$$\dot{R} = -R_x \gamma R y + R_y \gamma (R - 1) y. \quad (15)$$

Note that, for a given time \hat{t} in which $R(x(\hat{t}), y(\hat{t})) = 1$, this equation, together with (5), implies that $\dot{R}(x(\hat{t}), y(\hat{t})) < 0$. This proves that all stationary points of $y(t)$ are local maxima. Hence, if $R(x_0, y_0) \leq 1$, it must be $R(x(t), y(t)) < 1$ for every $t > 0$, so that $y(t)$ is necessarily strictly decreasing for every positive time $t \geq 0$, proving item (i). To prove

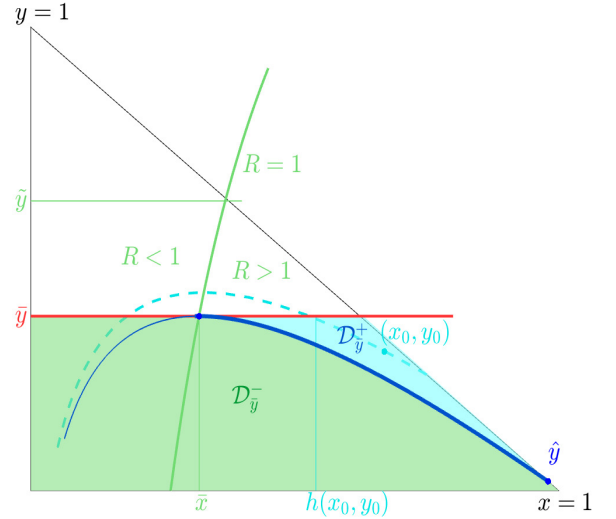


Fig. 2: Phase portrait of the uncontrolled BF-SIR model (14) on the state space \mathcal{S} , with recovery rate $\gamma = 0.05$ and infection rate (8) with $b(x) = (x + 2)/10$ and $a = 0.5$.

item (ii), let $R(x_0, y_0) > 1$ and assume by contradiction that $R(x(t), y(t)) > 1$ for every $t \geq 0$. Then, $y(t)$ would be strictly increasing for all times and could not converge to an equilibrium point, contradicting Proposition 1(iv). Therefore, $\hat{t} = \min\{t \geq 0 \mid R(x(t), y(t)) = 1\}$ must exist and has to be finite, otherwise the fraction of recovered agents would diverge in time due to the third equation in (1), violating Proposition 1. Hence, $y(t)$ is strictly increasing in $[0, \hat{t}]$. For $t \geq \hat{t}$, item (i) implies that $y(t)$ is strictly decreasing, proving item (ii). ■

B. Some geometric considerations

We analyze the dynamics of the uncontrolled BF-SIR model (14) in presence of a threshold \bar{y} in $(0, 1]$. Our goal is to determine which trajectories remain below this threshold without requiring external intervention.

It follows from [1, Chapter 2] that, for every initial condition (x_0, y_0) in \mathcal{S} , the uncontrolled BF-SIR model (14) admits a unique solution of class \mathcal{C}^1 in \mathcal{S} . Consequently, there exists a map $\phi : \mathbb{R}_+ \times \mathcal{S} \rightarrow \mathcal{S}$ such that $(x_0, y_0) \mapsto \phi(t, x_0, y_0)$ and $t \mapsto \phi(t, x_0, y_0)$ are both of class \mathcal{C}^1 and $t \mapsto \phi(t, x_0, y_0)$ is the unique solution of the uncontrolled BF-SIR model (14) with $\phi(0; x_0, y_0) = (x_0, y_0)$ in \mathcal{S} . The positive semi-orbit for the initial condition (x_0, y_0) is then defined as

$$\Gamma^+(x_0, y_0) = \{\phi(t, x_0, y_0), t \in \mathbb{R}_+\}.$$

For every state (x, y) in \mathcal{S} , we also define the set

$$\Gamma^-(x, y) = \{(x_0, y_0) \in \mathcal{S} : (x, y) \in \Gamma^+(x_0, y_0)\},$$

of initial conditions in \mathcal{S} whose positive semi-orbit contains (x, y) . With a slight abuse of terminology, we shall refer to $\Gamma^-(x, y)$ as the negative semi-orbit of (x, y) for the uncontrolled BF-SIR model (14).

Let $\mathcal{D}_{\bar{y}}$ denote the set of states that the trajectory can visit without violating the threshold constraint, that is

$$\mathcal{D}_{\bar{y}} = \{(x, y) \in \mathcal{S} : 0 < y \leq \bar{y}\}.$$

The first part of our analysis leads to a decomposition of $\mathcal{D}_{\bar{y}}$ into two sets $\mathcal{D}_{\bar{y}}^-$ and $\mathcal{D}_{\bar{y}}^+$, which will be formally defined after Lemma 2. Informally, $\mathcal{D}_{\bar{y}}^-$ contains the initial conditions from which the fraction of infected remains below the threshold \bar{y} without requiring an external intervention and is the largest positively invariant set contained in $\mathcal{D}_{\bar{y}}$, as established by Lemma 3. In contrast, $\mathcal{D}_{\bar{y}}^+$ contains all initial conditions such that the solution of the uncontrolled dynamics would exceed the threshold \bar{y} , thus requiring an external intervention. The two regions are illustrated in Figure 2.

The following statement characterizes the set of states such that $R(x, y) = 1$ and is instrumental for the definition of such sets.

Lemma 1: Let Assumption 1 hold true and assume that

$$\beta(1, 0) > \gamma. \quad (16)$$

Then, there exists a unique $\tilde{y} > 0$ such that $R(1 - \tilde{y}, \tilde{y}) = 1$ and a \mathcal{C}^1 function $\kappa : [0, \tilde{y}] \rightarrow [0, 1]$ such that

$$\{(x, y) \in \mathcal{S} : R(x, y) = 1\} = \{(\kappa(y), y) : y \in [0, \tilde{y}]\}.$$

Proof: Note from (3) that $R(0, 1) = 0$, while $R(1, 0) > 1$ due to (16). Therefore, since $y \mapsto R(1 - y, y)$ is continuous on $[0, 1]$, there exists \tilde{y} in $(0, 1)$ such that $R(1 - \tilde{y}, \tilde{y}) = 1$. For every $y \in [0, \tilde{y}]$, note that $R(0, y) = 0$ by (3). Moreover, for every such y , since $R(1 - \tilde{y}, \tilde{y}) = 1$, it follows from (5)-(6) that $R(1 - y, y) \geq 1$. Therefore, (5) implies the existence of a unique $x = \kappa(y)$ such that $R(\kappa(y), y) = 1$. The fact that κ is of class \mathcal{C}^1 follows from the Implicit Function Theorem [42, Theorem 9.18] and from (5). ■

Remark 2: The function κ maps y in $[0, \tilde{y}]$ into the unique fraction of susceptible agents $\kappa(y)$ in $[0, 1 - y]$ such that $R(\kappa(y), y) = 1$. In the classical SIR model, $\tilde{y} = 1 - \gamma/\beta$ and $\kappa(y) = \gamma/\beta$ for every y in $[0, \tilde{y}]$.

Figure 2 illustrates in green the curve $x = \kappa(y)$. Due to the monotonicity of the reproduction number, this curve splits \mathcal{S} in two areas, the left-hand one with $R(x, y) < 1$ and the right-hand one with $R(x, y) > 1$.

Now, let $\bar{x} = \kappa(\bar{y})$. It is useful in our analysis to consider the negative semi-orbit $\Gamma^-(\bar{x}, \bar{y})$ for the uncontrolled BF-SIR model (14). The following result gives information on $\Gamma^-(\bar{x}, \bar{y})$ and permits the definition of $\mathcal{D}_{\bar{y}}^+$ and $\mathcal{D}_{\bar{y}}^-$.

Lemma 2: Let Assumption 1 and (16) hold true and assume that $\bar{y} \leq \tilde{y}$. Then, there exists \hat{y} in $[0, \bar{y}]$ and a \mathcal{C}^1 decreasing function $\lambda : [\hat{y}, \bar{y}] \rightarrow [\bar{x}, 1]$ such that:

- (i) $\Gamma^-(\bar{x}, \bar{y}) = \{(\lambda(y), y) : \hat{y} \leq y \leq \bar{y}\}$;
- (ii) there exists (x, y) in $\Gamma^-(\bar{x}, \bar{y})$ with $x + y = 1$ if and only if $\hat{y} > 0$. In such a case, \hat{y} is the unique element in $(0, \bar{y}]$ such that $\lambda(\hat{y}) + \hat{y} = 1$;
- (iii) $\lambda(y) > \kappa(y)$ for every y in $[\hat{y}, \bar{y}]$ and $\lambda(\bar{y}) = \kappa(\bar{y}) = \bar{x}$. In particular, $R(\lambda(y), y) > 1$ for every $[\hat{y}, \bar{y}]$;

Proof: We define the dynamics

$$\begin{cases} \dot{x} = \beta(x, y)xy, \\ \dot{y} = -\beta(x, y)xy + \gamma y. \end{cases} \quad (17)$$

and let $(x(t), y(t)) = \phi^-(t, \bar{x}, \bar{y})$ denote the unique solution of (17) at time t in \mathbb{R}_+ with initial condition $(x(0), y(0)) = (\bar{x}, \bar{y})$. Note that (17) is obtained from (14) by letting $t \rightarrow -t$, so that

$$\Gamma^-(\bar{x}, \bar{y}) = \{\phi^-(t, \bar{x}, \bar{y}) : t \in \mathbb{R}_+\}. \quad (18)$$

Note that $R(x(0), y(0)) = R(\bar{x}, \bar{y}) = 1$. Hence, Proposition 2 and (18) imply that necessarily

$$R(x(t), y(t)) > 1, \quad \forall t > 0. \quad (19)$$

Therefore, the trajectory enters the set of points with reproduction number larger than 1 for positive times t and this set can be left only if the trajectory leaves \mathcal{S} (we remark that \mathcal{S} is not positively invariant under the backward dynamics). This in turn implies that $y(t)$ is strictly decreasing, while $x(t)$ is strictly increasing. Now, note that either $(x(t), y(t))$ belongs to \mathcal{S} for all positive times t , in which case the solution converges to a point in the boundary of \mathcal{S} as $t \rightarrow +\infty$, or it hits the boundary of \mathcal{S} at some finite time. Let us indicate the convergence or hit point by (\hat{x}, \hat{y}) . We note that, in the first case, such point must be an equilibrium, so that necessarily $\hat{y} = 0$ from Proposition (1) (note that the equilibrium points of the backward dynamics coincide with the ones of the original dynamics). In the second case, instead, such a point (\hat{x}, \hat{y}) must lie on the boundary of \mathcal{S} , with \hat{y} in $(0, \bar{y}]$ and $\hat{x} = 1 - \hat{y}$, so that $\hat{x} + \hat{y} = 1$. In both cases, the strict monotonicity of $y(t)$ ensures that the first component of the orbit $\Gamma^-(\bar{x}, \bar{y})$ can be represented as the graph of a function of y , denoted $\lambda(y) := x(y)$ and defined on $[\hat{y}, \bar{y}]$. By construction, the function λ is of class \mathcal{C}^1 since both $x(t)$ and $y(t)$ are \mathcal{C}^1 and $y(t)$ is strictly decreasing. Moreover, λ is a strictly decreasing function because the strict monotonicity of $x(t)$ and $y(t)$ implies $dx/dy = \dot{x}/\dot{y} < 0$. This proves item (i). Item (ii) follows from the fact that $\hat{y} > 0$ if and only if $(x(t), y(t))$ hits the boundary of \mathcal{S} , so that necessarily $\lambda(\hat{y}) + \hat{y} = 1$. The fact that $\lambda(\bar{y}) = \kappa(\bar{y}) = \bar{x}$ follows by construction. The fact that $R(\lambda(y), y) > 1$ for every $[\hat{y}, \bar{y}]$ follows from (19), proving item (iii). ■

The negative semi-orbit $\Gamma^-(\bar{x}, \bar{y})$ is represented by the thick blue curve in Figure 2. The green and the light-blue area are, respectively, the sets $\mathcal{D}_{\bar{y}}^-$ and $\mathcal{D}_{\bar{y}}^+$. If the negative semi-orbit that starts from (\bar{x}, \bar{y}) intercepts a point (x, y) on the upper-right boundary of \mathcal{S} , then $\hat{y} > 0$, otherwise $\hat{y} = 0$.

Lemma 2 allows for the partition of $\mathcal{D}_{\bar{y}}$ in two subsets

$$\begin{aligned} \mathcal{D}_{\bar{y}}^+ &= \{(x, y) \in \mathcal{D}_{\bar{y}} : y \in [\hat{y}, \bar{y}], x > \lambda(y)\}, \\ \mathcal{D}_{\bar{y}}^- &= \mathcal{D}_{\bar{y}} \setminus \mathcal{D}_{\bar{y}}^+. \end{aligned} \quad (20)$$

Remark 3: Note that, since $R(\lambda(y), y) > 1$ for every y in $[\hat{y}, \bar{y}]$ by Lemma 2(iii) and since $R(\bar{x}, \bar{y}) = 1$, $\mathcal{D}_{\bar{y}}^+$ contains all points with reproduction number larger than 1 due to the monotonicity condition (6). Therefore, this yields that $\rho(x, y) > 0$ for all (x, y) in $\mathcal{D}_{\bar{y}}^+$.

Remark 4: Let Assumption 1 hold true. Then, if (16) does not hold true, \tilde{y} and \hat{y} are not defined and $R(x, y) \leq 1$ for every (x, y) in \mathcal{S} . Hence, the set $\mathcal{D}_{\bar{y}}^+$ is empty by Remark 3 and $\mathcal{D}_{\bar{y}} = \mathcal{D}_{\bar{y}}^-$. Furthermore, the set $\mathcal{D}_{\bar{y}}^+$ is empty if and only if $R(1 - \bar{y}, \bar{y}) \leq 1$. If (16) holds true, this is equivalent to $\bar{y} \leq \tilde{y}$.

If in particular $\tilde{y} < \bar{y}$, then \bar{x} does not exist, therefore neither \hat{y} and the function λ are well defined. If instead $\tilde{y} = \bar{y}$, then $\bar{x} = 1 - \bar{y}$, $\hat{y} = \tilde{y} = \bar{y}$ and the curve $x = \lambda(y)$ degenerates to a point $(1 - \bar{y}, \bar{y})$.

C. Dynamic behavior of the uncontrolled BF-SIR epidemic model

In this part, we discuss the behavior of the uncontrolled BF-SIR epidemic model (14) with initial conditions either in $\mathcal{D}_{\bar{y}}^-$ or in $\mathcal{D}_{\bar{y}}^+$. In the first case, we show that the orbit remains inside $\mathcal{D}_{\bar{y}}^-$ and thus, in particular, the number of infected agents never exceeds \bar{y} . In this case, $u \equiv 0$ for all t , is the optimal control. In contrast, if the initial condition lies in $\mathcal{D}_{\bar{y}}^+$, the trajectory will leave $\mathcal{D}_{\bar{y}}$ at some finite time, violating the threshold constraint. We also show that the abscissa of the hitting point is a regular function of the initial condition, a fact that will play a crucial role in the proof of Theorem 1.

Lemma 3: Let Assumption 1 hold true. Then, the set $\mathcal{D}_{\bar{y}}^-$ is positively invariant for the uncontrolled BF-SIR epidemic model (14).

Proof: Let $\mathcal{I} = \{(x, \bar{y}) \in \mathcal{S} : x \leq \bar{x}\}$. Since \mathcal{S} is positively invariant by Proposition 1 a solution $(x(t), y(t))$ can exit $\mathcal{D}_{\bar{y}}^-$ by crossing either $\Gamma^-(\bar{x}, \bar{y})$ or \mathcal{I} . The first option is not possible for the uniqueness of the solution of the ODE. Since $R(\bar{x}, \bar{y}) = 1$ by construction, it follows from (5) that $R(x, y) < 1$ for every point $(x, y) \in \mathcal{I}$. Hence, the trajectory cannot leave $\mathcal{D}_{\bar{y}}^-$ by crossing \mathcal{I} . This concludes the proof. ■

Lemma 4: Let β be of class \mathcal{C}^2 and let Assumption 1 hold true. Then:

- (i) for every (x, y) in $\mathcal{D}_{\bar{y}}^+$, there exists a finite time t such that $\phi(t, x, y)$ does not belong to $\mathcal{D}_{\bar{y}}$;
- (ii) for every (x, y) in $\mathcal{D}_{\bar{y}}^+$, there exists a \mathcal{C}^2 map $h : \mathcal{D}_{\bar{y}}^+ \rightarrow (\bar{x}, 1 - \bar{y}]$ such that $(h(x, y), \bar{y})$ belongs to $\Gamma(x, y)$ and $h(x, y) \leq x$, where equality holds true if and only if $y = \bar{y}$;
- (iii) for every (x_0, y_0) in $\Gamma^-(\bar{x}, \bar{y})$,

$$\lim_{\substack{(x, y) \rightarrow (x_0, y_0) \\ (x, y) \in \mathcal{D}_{\bar{y}}^+}} h(x, y) = \bar{x}. \quad (21)$$

- (iv) h is a constant of motion of the uncontrolled BF-SIR epidemic model (14) in $\mathcal{D}_{\bar{y}}^+$, that is, $h(x, y) = \xi$ for every (x, y) in $\Gamma^-(\xi, \bar{y})$ with ξ in $(\bar{x}, 1 - \bar{y}]$;

Proof: (i) Recall from Remark 3 that $R(x, y) > 1$ for every (x, y) in $\mathcal{D}_{\bar{y}}^+$. This implies that every trajectory in $\mathcal{D}_{\bar{y}}^+$ is such that $y(t)$ is strictly increasing in t as long as the solution remains in $\mathcal{D}_{\bar{y}}^+$. It thus follows from Proposition 2(ii) that the solution must necessarily exit $\mathcal{D}_{\bar{y}}^+$ in finite time. Since \mathcal{S} is positively invariant by Proposition 1, the trajectory can leave $\mathcal{D}_{\bar{y}}^+$ by crossing either $\Gamma^-(\bar{x}, \bar{y})$ or the set

$$\mathcal{J} = \{(x, \bar{y}) \in \mathcal{S} : \bar{x} < x \leq 1 - \bar{y}\}. \quad (22)$$

Since $\Gamma^-(\bar{x}, \bar{y})$ cannot be crossed because of the uniqueness of the solutions, the trajectory must necessarily cross \mathcal{J} in finite time. This implies that the trajectory leaves $\mathcal{D}_{\bar{y}}$ in finite time.

- (ii) Given (x_0, y_0) in $\mathcal{D}_{\bar{y}}^+$ and $t \geq 0$, we let

$$\phi(t, x_0, y_0) = (x(t, x_0, y_0), y(t, x_0, y_0))$$

to be the solution of (14) at time t with initial condition (x_0, y_0) . Now, note that, since the right hand side of (14) is of class \mathcal{C}^2 , ϕ is of class \mathcal{C}^2 both in t and in (x_0, y_0) . We now define $T(x_0, y_0)$ to be the minimum time t for which $\phi(t, x_0, y_0) \in \mathcal{J}$, well defined because of item (i), and define $h : \mathcal{D}_{\bar{y}}^+ \rightarrow (\bar{x}, 1 - \bar{y}]$ by putting

$$h(x_0, y_0) = x(T(x_0, y_0), x_0, y_0).$$

Note that, for every (x_0, y_0) in $\mathcal{D}_{\bar{y}}^+$, $y(T(x_0, y_0), x_0, y_0) = \bar{y}$ by construction and $\dot{y}(T(x_0, y_0), x_0, y_0) > 0$ because of Remark 3. A direct application of the Implicit Function Theorem [42, Theorem 9.18] (on all points of $\mathcal{D}_{\bar{y}}^+$ including the boundary segment \mathcal{J}) together with the regularity of ϕ yields that T is of class \mathcal{C}^2 . Finally, the \mathcal{C}^2 regularity of h follows from the analogous regularity of T and ϕ . Note also that $\dot{x}(T(x_0, y_0), x_0, y_0) \leq 0$ for every (x_0, y_0) in $\mathcal{D}_{\bar{y}}^+$ from Proposition 1(i), and together with $x(T(x_0, y_0), x_0, y_0) \leq x_0$ leads to $h(x_0, y_0) \leq x_0$.

(iv) The fact that h is a constant of motion of (14) is a consequence of its definition, since the trajectories that start from points that belong to the same negative semi-orbit will hit segment \mathcal{J} in the same point because of the uniqueness of the solutions.

(iii) If $(x_0, y_0) = (\bar{x}, \bar{y})$, the thesis is straightforward: fixed an arbitrary $\epsilon > 0$, for every $(x, y) \in B_\epsilon(x_0, y_0) \cap \mathcal{D}_{\bar{y}}^+$ we have that, thanks to the definition of h and item (ii),

$$\bar{x} < h(x, y) \leq x \leq \bar{x} + \epsilon$$

This yields relation (21).

Consider now (x_0, y_0) in $\Gamma^-(\bar{x}, \bar{y}) \setminus \{(\bar{x}, \bar{y})\}$ and let $T(x_0, y_0) > 0$ be the time such that $\phi(T(x_0, y_0), x_0, y_0) = (\bar{x}, \bar{y})$. Fix any positive $\epsilon < \|(\bar{x}, \bar{y}) - (x_0, y_0)\|$ and let $T_\epsilon < T(x_0, y_0)$ be such that

$$\|\phi(T_\epsilon, x_0, y_0) - (\bar{x}, \bar{y})\| = \epsilon/2 \quad (23)$$

Such a time T_ϵ exists because of the continuity of the solution and it holds that $\epsilon_y = \bar{y} - y(T_\epsilon, x_0, y_0) \in (0, \epsilon/2)$. By regularity with respect to the initial condition, there exists $\delta > 0$ such that, for every $(x_\delta, y_\delta) \in B_\delta(x_0, y_0) \cap \mathcal{D}_{\bar{y}}^+$,

$$\|\phi(t, x_0, y_0) - \phi(t, x_\delta, y_\delta)\| < \epsilon_y \quad \forall t \in [0, T_\epsilon] \quad (24)$$

This implies that $\phi(t, x_\delta, y_\delta)$ belongs to $\mathcal{D}_{\bar{y}}^+$ for all $t \in [0, T_\epsilon]$. As a consequence of item (ii), we thus have that

$$h(\phi(T_\epsilon, x_\delta, y_\delta)) \leq x(T_\epsilon, x_\delta, y_\delta). \quad (25)$$

Hence,

$$\begin{aligned} \bar{x} &< h(x_\delta, y_\delta) = h(\phi(T_\epsilon, x_\delta, y_\delta)) \\ &\leq x(T_\epsilon, x_\delta, y_\delta) < \bar{x} + \epsilon/2 + \epsilon/2 = \bar{x} + \epsilon, \end{aligned}$$

where the first inequality follows from the definition of h , the first equality from item (iv), the second inequality from (25) and the last inequality from (23)-(24). Because of the arbitrariness of $\epsilon > 0$, this yields the limit relation (21). ■

Remark 5: The quantity $h(x, y)$ is the abscissa of the crossing point of the orbit that starts from (x, y) in $\mathcal{D}_{\bar{y}}^+$ with segment \mathcal{J} , i.e. the fraction of susceptible agents reached by the dynamics when the fraction of infected agents hits the threshold \bar{y} . An example of trajectory that starts in $\mathcal{D}_{\bar{y}}^+$ is illustrated in Figure 2 by the light-blue dashed curve.

We now establish a technical result that characterizes the function h .

Lemma 5: Let β be of class \mathcal{C}^2 and let Assumption 1 hold true. Then, for every (x, y) in $\mathcal{D}_{\bar{y}}^+$:

$$(i) \quad h_x(x, y)R(x, y) = h_y(x, y)(R(x, y) - 1); \quad (26)$$

$$(ii) \quad 0 \leq h_y(x, y) \leq \frac{1}{\rho(h(x, y), \bar{y})}; \quad (27)$$

$$(iii) \text{ if } y = \bar{y}, \quad h_y(x, y) = \frac{1}{\rho(h(x, y), \bar{y})}.$$

Proof: (i) It follows from Lemma 4(iv) that $\dot{h} = h_x \dot{x} + h_y \dot{y} = 0$ for every (x, y) in $\mathcal{D}_{\bar{y}}^+$ under the uncontrolled BF-SIR model (14). Using (14), we then get item (i).

(ii)-(iii) We now show that $h_x(x, y) \geq 0$ on $\mathcal{D}_{\bar{y}}^+$. For (x_0, y_0) in $\mathcal{D}_{\bar{y}}^+$, choose $\epsilon > 0$ such that $(x_0 - \epsilon, y_0)$ belongs to $\mathcal{D}_{\bar{y}}^+$. Denote by $(x(t), y(t))$ and $(x_\epsilon(t), y_\epsilon(t))$ the solutions associated with initial conditions (x_0, y_0) and $(x_0 - \epsilon, y_0)$, respectively. As long as they remain in $\mathcal{D}_{\bar{y}}^+$, the second components $y(t)$ and $y_\epsilon(t)$ are both increasing in time, so that the corresponding orbits can be described as graphicals of functions, denoted respectively $x = f(y)$ and $x = f_\epsilon(y)$ with y in $[y_0, \bar{y}]$. Since the orbits cannot intersect and since $x_0 = f(y_0) > x_0 - \epsilon = f_\epsilon(y_0)$, it must be $h(x_0, y_0) = f(\bar{y}) > f_\epsilon(\bar{y}) = h(x_0 - \epsilon, \bar{y})$. Given the arbitrariness of ϵ , this implies that $h_x(x_0, y_0) \geq 0$. Moreover, since $x \mapsto h(x, \bar{y})$ is the identity function on $(\bar{x}, 1]$, we have that $h_x(x, \bar{y}) = 1$. Consequently, thanks to (26) and thanks to the fact that $R(x, y) > 1$ for every (x, y) in $\mathcal{D}_{\bar{y}}^+$ because of Remark 3, we also have that

$$h_y(x, y) \geq 0 \quad \forall (x, y) \in \mathcal{D}_{\bar{y}}^+, \quad (28)$$

$$h_y(x, \bar{y}) = \frac{R(x, \bar{y})}{R(x, \bar{y}) - 1} = \frac{1}{\rho(x, \bar{y})}. \quad (29)$$

Since $h(x, y) = x$ whenever $y = \bar{y}$, (29) proves item (iii), while (28) proves the left hand inequality of item (ii). To conclude the proof of item (ii), note that

$$\begin{aligned} \dot{h}_y &= \dot{x} h_{xy} + \dot{y} h_{yy} \\ &= -R\gamma y h_{xy} + (R - 1)\gamma y h_{yy}. \end{aligned} \quad (30)$$

Taking the partial derivative of (26) with respect to y and then substituting (26) inside this derivative, we get

$$\begin{aligned} h_{xy}R &= h_{yy}(R - 1) + (h_y - h_x)R_y \\ &= h_{yy}(R - 1) + R^{-1}h_yR_y. \end{aligned}$$

Plugging this expression into (30) we finally get

$$\dot{h}_y = -\gamma y R^{-1} h_y R_y \geq 0, \quad (31)$$

whose sign follows from (6) and (28). Since h_y is non-decreasing in time by (31) and since $(h(x, y), \bar{y})$ belongs to the positive orbit $\Gamma(x, y)$, we get that

$$h_y(x, y) \leq h_y(h(x, y), \bar{y}).$$

for every (x, y) in $\mathcal{D}_{\bar{y}}^+$. Combining this with (29) we obtain the thesis. ■

Remark 6: Lemma 4 and Lemma 5 guarantee the existence of $h(x, y)$ for every (x, y) in $\mathcal{D}_{\bar{y}}^+$ under conditions (5)-(6) and characterize $h(x, y)$. Although its existence and regularity is essential to prove our main result, the explicit form of $h(x, y)$ cannot be found unless in some special cases. For instance, the explicit form of $h(x, y)$ may be found for the classical SIR epidemic model and for the BF-SIR epidemic model with feedback mechanism of Example 1, due to the fact that the BF-SIR epidemic model with such feedback mechanism and the classical SIR model admit a non-trivial invariant of motion. We refer to [41], [39] for more details.

IV. PROOF OF OPTIMALITY

In this section we provide the proof of Theorem 1. This is obtained by first giving a characterization of the candidate value function in Section IV-A (i.e., the cost of the candidate optimal control) and then proving optimality in Section IV-B.

A. Candidate value function

In this section, we compute the cost of the candidate optimal control signal $u^*(t)$ defined in (11)–(12).

We start with a simple preliminary result that characterizes the dynamics under the optimal control and the associated cost, when the optimal control is not the trivial control signal $u^* \equiv 0$. As pointed out in Remark 4, if (16) is not verified, or if (16) holds true and $\bar{y} \leq \bar{y}$ (cf. Lemma 1 for the definition of \bar{y}), then $\mathcal{D}_{\bar{y}}^- = \mathcal{D}_{\bar{y}}$, so that the optimal control is $u^* \equiv 0$ by Lemma 3. Hence, in the next part we shall work under the assumption that (16) holds true and $\bar{y} > \bar{y}$. We let $T_0 = T(x_0, y_0)$ be the first time the solution of (14) with initial condition (x_0, y_0) in $\mathcal{D}_{\bar{y}}^+$ hits the threshold \bar{y} and let

$$T_1 = T_0 + \frac{h(x_0, y_0) - \bar{x}}{\gamma \bar{y}},$$

where the function h was introduced in Lemma 4.

Proposition 3: Let Assumption 1 hold true and assume that a threshold \bar{y} and an initial condition (x_0, y_0) in $\mathcal{D}_{\bar{y}}^+$ have been fixed. Consider the control function

$$u^*(t) = \begin{cases} 0 & \text{if } t < T_0 \text{ or } t > T_1 \\ \rho(\tilde{x}(t), \bar{y}) & \text{if } T_0 \leq t \leq T_1 \end{cases} \quad (32)$$

where

$$\tilde{x}(t) = h(x_0, y_0) - \gamma(t - T_0)\bar{y}.$$

Then the corresponding solution of the CBF-SIR epidemic model (4) $(x^*(t), y^*(t))$ has the following properties:

(i) $(x^*(t), y^*(t))$ admits the following form for $T_0 < t < T_1$:

$$\begin{cases} x^*(t) = h(x_0, y_0) - \gamma(t - T_0)\bar{y}, \\ y^*(t) = \bar{y}. \end{cases} \quad (33)$$

- (ii) The feedback relation $u^*(t) = \mu(x^*(t), y^*(t))$ holds for every $t \geq 0$.
- (iii) u^* is feasible, namely $y^*(t) \leq \bar{y}$ for every $t \geq 0$.
- (iv) The cost of u^* is given by

$$J(u^*) = \frac{1}{\gamma \bar{y}} \int_{\bar{x}}^{h(x_0, y_0)} \rho(x, \bar{y}) dx.$$

Proof: (i) By construction, up to time T_0 the evolution of the CBF-SIR epidemic model (4) coincides with the uncontrolled case. By the way T_0 is defined, it then follows that

$$(x^*(T_0), y^*(T_0)) = (h(x_0, y_0), \bar{y}).$$

We observe that the vector function in (33) coincides with $(x^*(T_0), y^*(T_0))$ for $t = T_0$. Moreover a direct check shows that such a vector function is a solution of (4) with control u^* in $[T_0, T_1]$. This proves item (i). Item (ii) is a direct consequence of the definition of μ and of item (i). To prove item (iii) notice that, by construction the inequality $y^*(t) \leq \bar{y}$ is satisfied till time T_1 . Notice now that the solution $(x^*(t), y^*(t))$ for $t > T_1$ coincides with the solution of the uncontrolled model with initial condition $x^*(T_1) = \bar{x}$ and $y^*(T_1) = \bar{y}$. Since $R(\bar{x}, \bar{y}) = 1$, it follows from Proposition 2(i) that $y^*(t)$ is strictly decreasing from this time on. This yields $y^*(t) < \bar{y}$ also for $t > T_1$ and proves item (iii). Finally,

$$\begin{aligned} J(u^*) &= \int_0^{+\infty} u^*(t) dt = \int_{T_0}^{T_1} u^*(t) dt \\ &= \int_{T_0}^{T_1} \rho(x^*(t), y^*(t)) dt = \int_{T_0}^{T_1} \rho(x^*(t), \bar{y}) dt \\ &= \frac{1}{\gamma \bar{y}} \int_{\bar{x}}^{h(x_0, y_0)} \rho(x, \bar{y}) dx, \end{aligned}$$

where the last two equivalences follow from item (i) by a change of variables. This proves item (iv) and concludes the proof. ■

Motivated by Proposition 3, we define our candidate value function $V : \mathcal{D}_{\bar{y}} \rightarrow \mathbb{R}$ by

$$V(x, y) = \begin{cases} 0 & \text{if } (x, y) \in \mathcal{D}_{\bar{y}}^- \\ \frac{1}{\gamma \bar{y}} \int_{\bar{x}}^{h(x, y)} \rho(s, \bar{y}) ds & \text{if } (x, y) \in \mathcal{D}_{\bar{y}}^+. \end{cases} \quad (34)$$

The following result provides some properties of the candidate value function that are instrumental for the proof of Theorem 1.

Lemma 6: Assume that β is a \mathcal{C}^2 function and let Assumption 1 hold true. Consider V defined in (34), then:

- (i) V is continuous on $\mathcal{D}_{\bar{y}}$ and \mathcal{C}^1 on $\mathcal{D}_{\bar{y}}^+$;
- (ii) for every (x, y) in $\mathcal{D}_{\bar{y}}^+$,

$$V_y(x, y) = \frac{\rho(h(x, y), \bar{y})}{\gamma \bar{y}} h_y(x, y), \quad (35)$$

$$V_x(x, y) = \rho(h(x, y), \bar{y}) V_y(x, y); \quad (36)$$

- (iii) $0 \leq V_y(x, y) \leq 1/(\gamma \bar{y})$ for every (x, y) in $\mathcal{D}_{\bar{y}}^+$;
- (iv) $V_y(x, y) = 1/(\gamma \bar{y})$ for every (x, y) in $\mathcal{D}_{\bar{y}}^+$ with $y = \bar{y}$.

Proof: (i) Note that $V(x, y) = 0$ for every (x, y) in $\Gamma^-(\bar{x}, \bar{y})$ since $\Gamma^-(\bar{x}, \bar{y})$ belongs to $\mathcal{D}_{\bar{y}}^-$. Moreover, it follows

from Lemma 4(iii) and from the Definition of V that for every (x, y) in $\Gamma^-(\bar{x}, \bar{y})$

$$\lim_{\substack{(x_0, y_0) \rightarrow (x, y) \\ (x_0, y_0) \in \mathcal{D}_{\bar{y}}^+}} V(x_0, y_0) = 0.$$

This, together with the continuity of $h(x, y)$ established in Lemma 4(i), proves continuity of V on $\mathcal{D}_{\bar{y}}$. The differentiability of V on $\mathcal{D}_{\bar{y}}^+$ follows from the differentiability of h established in Lemma 4(ii).

(ii) The statement follows from (34) and (26) by direct computation.

(iii) The fact that $V_y(x, y) \geq 0$ follows from item (ii), from Lemma 5(ii) and from the fact that $\rho(x, y) \geq 0$ for every (x, y) in $\mathcal{D}_{\bar{y}}^+$ by Remark 3. The right-hand inequality follows immediately from Lemma 5(ii).

(iv) The statement is a straightforward consequence of Lemma 5(iii). ■

Remark 7: Note that since h is a constant of motion of the uncontrolled BF-SIR epidemic model (14) in $\mathcal{D}_{\bar{y}}^+$ (cf. Lemma 4(iv)), the same property also holds for V .

Lemma 6 states that the candidate value function $V(x, y)$ is continuous on $\mathcal{D}_{\bar{y}}$, but continuously differentiable on $\mathcal{D}_{\bar{y}}^+$ only. In fact, it is not hard to prove that $V(x, y)$ is not continuously differentiable on $\Gamma^-(\bar{x}, \bar{y})$. For this reason, we cannot apply the Hamilton-Jacobi-Bellman equation [43], [44] to prove that u^* is the optimal control. In the next section we shall provide an alternative prove for our main result.

B. Proof of Theorem 1

The next result proves that, for every feasible control with finite cost, the CBF-SIR model (4) enters the region with reproduction number less than one in finite time.

Lemma 7: Let u in $\mathcal{U}_{x_0, y_0}^{\bar{y}}$ be such that $J(u) < +\infty$, and let $(x(t), y(t))$ be the corresponding solution of the CBF-SIR epidemic model (4) with initial condition (x_0, y_0) in $\mathcal{D}_{\bar{y}}$. Then, there exists a finite time \bar{t} such that $R(x(\bar{t}), y(\bar{t})) < 1$.

Proof: Assume by contradiction that $R(x(t), y(t)) \geq 1$ for every time t and let \hat{R} be the maximum of the function R over the compact set \mathcal{S} . Integrating the second equation in (4) and using the inequality

$$(1 - u(t))R(x(t), y(t)) - 1 \geq -u(t)R(x(t), y(t)) \geq -u(t)\hat{R}$$

yields

$$\begin{aligned} y(t) &= y_0 \exp \left(\gamma \int_0^t ((1 - u(\tau))R(x(\tau), y(\tau)) - 1) d\tau \right) \\ &\geq y_0 \exp \left(\gamma \hat{R} \int_0^t (-u(\tau)) d\tau \right). \end{aligned}$$

Since $\lim_{t \rightarrow +\infty} y(t) = 0$ by Proposition 1(iv), we get that

$$J(u) = \lim_{t \rightarrow +\infty} \int_0^t u(\tau) d\tau = +\infty,$$

proving the statement. ■

We can now proceed to prove Theorem 1.

If (x_0, y_0) belongs to $\mathcal{D}_{\bar{y}}^-$, the uncontrolled solution remains below \bar{y} at all times thanks to Lemma 3. Therefore $u \equiv 0$ is an optimal control that satisfies Theorem 1.

We now assume that (x_0, y_0) belongs to $\mathcal{D}_{\bar{y}}^+$ and we show that the control signal defined in (32) is optimal.

To this end, consider a feasible control u in $\mathcal{U}_{x_0, y_0}^{\bar{y}}$ such that $J(u) < +\infty$ and let $(x^u(t), y^u(t))$, for $t \geq 0$, be the solution of (4) with such control signal and initial state (x_0, y_0) . Since $R(x, y) > 1$ for every (x, y) in $\mathcal{D}_{\bar{y}}^+$ by Remark 3, the solution $(x^u(t), y^u(t))$ must exit $\mathcal{D}_{\bar{y}}^+$ at some finite time because of Lemma 7 and because $J(u) < +\infty$. By the way $\mathcal{D}_{\bar{y}}^+$ is defined (equations (20)), it follows that the boundary of this subset in the positively invariant set \mathcal{S} consists of the graphical of λ and of interval \mathcal{J} defined in (22). As u is assumed to be feasible, necessarily the exit point must be located in the graphical of λ . In other words, there exists a finite time t° such that

$$y^u(t^\circ) \leq \bar{y}, \quad x^u(t^\circ) = \lambda(y^u(t^\circ)), \quad (37)$$

$$(x^u(t), y^u(t)) \in \mathcal{D}_{\bar{y}}^+ \quad \forall t < t^\circ. \quad (38)$$

Let u° be the control signal defined as

$$u^\circ(t) = \begin{cases} u(t) & t \in [0, t^\circ) \\ 0 & t \in [t^\circ, +\infty) \end{cases}, \quad (39)$$

and let $(x^\circ(t), y^\circ(t))$, for $t \geq 0$, be the solution of (4) with control signal u° and initial state (x_0, y_0) . Since u is piecewise- \mathcal{C}^1 , also u° , by construction, is piecewise- \mathcal{C}^1 . The solution $(x^\circ(t), y^\circ(t))$ coincides with $(x^u(t), y^u(t))$ on $[0, t^\circ]$ while coincides with a trajectory of the uncontrolled model for $t > t^\circ$ with an initial condition $(x^u(t^\circ), y^u(t^\circ))$. In particular, since $(x^\circ(t^\circ), y^\circ(t^\circ))$ belongs to $\mathcal{D}_{\bar{y}}^-$, Lemma 3 guarantees that $(x^\circ(t), y^\circ(t))$ belongs to $\mathcal{D}_{\bar{y}}^-$ for all times $t \geq t^\circ$. This yields $y^\circ(t) \leq \bar{y}$ for all times t . In other terms, the control u° is feasible. Moreover,

$$\begin{aligned} J(u^\circ) &= \int_0^{+\infty} u^\circ(t) dt = \int_0^{t^\circ} u^\circ(t) dt \\ &= \int_0^{t^\circ} u(t) dt \leq \int_0^{+\infty} u(t) dt = J(u). \end{aligned} \quad (40)$$

In the following, we compare the candidate optimal control u^* with the control u° . In order to do this, we need to preliminarily study the regularity of the composed function $V(x^\circ(t), y^\circ(t))$. Because of property (38) and Lemma 6(i), we have that $V(x^\circ(t), y^\circ(t))$ is piecewise- \mathcal{C}^1 on $[0, t^\circ)$ and, trivially, on $(t^\circ, +\infty)$. Moreover, for every $t < t^\circ$ where the derivative exists, it satisfies

$$\begin{aligned} \dot{V}(x^\circ(t), y^\circ(t)) &= V_x(x^\circ, y^\circ)\dot{x}^\circ + V_y(x^\circ, y^\circ)\dot{y}^\circ \\ &= (\rho(h(x^\circ, y^\circ), \bar{y})\dot{x}^\circ + \dot{y}^\circ)V_y(x^\circ, y^\circ) \end{aligned} \quad (41)$$

where the second equality follows from (36). Because of Definition (10) and Assumption 1, the function $\rho(x, y)$ is increasing in x and decreasing in y . Since $h(x^\circ(t), x^\circ(t)) \leq x^\circ(t)$ by Lemma 4(ii) and $y^\circ(t) \leq \bar{y}$ for every $t \leq t^\circ$, we thus have

$$\rho(h(x^\circ(t), y^\circ(t)), \bar{y}) \leq \rho(x^\circ(t), y^\circ(t)). \quad (42)$$

Hence, for every t in $[0, t^\circ)$ where the derivative exists, we get

$$\begin{aligned} \dot{V}(x^\circ(t), y^\circ(t)) &\geq (\rho(x^\circ, y^\circ)\dot{x}^\circ + \dot{y}^\circ)V_y(x^\circ, y^\circ) \\ &= -\gamma y^\circ(t)u^\circ(t)V_y(x^\circ(t), y^\circ(t)) \\ &\geq -\frac{y^\circ(t)}{\bar{y}}u^\circ(t) \\ &\geq -u^\circ(t) \end{aligned} \quad (43)$$

where the first inequality follows from (41)-(42) and from the left-hand inequality of Lemma 6(iii), the equality from (4), the second inequality from the right-hand inequality of Lemma 6(iii) and the last one from the feasibility of u° . On the other hand, (34) implies that

$$\dot{V}(x^\circ(t), y^\circ(t)) = 0 = u^\circ(t), \quad \forall t > t^\circ, \quad (44)$$

since $(x^\circ(t), y^\circ(t))$ belongs to $\mathcal{D}_{\bar{y}}^-$ for such times.

We now derive an upper bound for $\dot{V}(x^\circ(t), y^\circ(t))$ for every t in $[0, t^\circ)$ where the derivative exists by

$$\begin{aligned} \dot{V}(x^\circ(t), y^\circ(t)) &\leq \dot{y}^\circ V_y(x^\circ, y^\circ) \\ &= \gamma y^\circ [R(x^\circ, y^\circ)(1 - u^\circ) - 1] V_y(x^\circ, y^\circ) \\ &\leq \gamma y^\circ R(x^\circ, y^\circ) V_y(x^\circ, y^\circ) \\ &\leq R(x^\circ(t), y^\circ(t)) \\ &\leq R(1, 0) \end{aligned} \quad (45)$$

where the first inequality follows from the monotonicity of $x^\circ(t)$ and the non-negativity of V_x , the equality from (4), the second inequality from the left-hand inequality of Lemma 6(iii) and from $(x^\circ, y^\circ) \in \mathcal{D}_{\bar{y}}^+$, which together with Remark 4 imply that $R(x^\circ, y^\circ)(1 - u^\circ) - 1 \leq R(x^\circ, y^\circ)$, the third one from the right-hand inequality of Lemma 6(iii) and the last one from Assumption 1. Inequalities (43) and (45) together with relation (44) yield that $\dot{V}(x^\circ(t), y^\circ(t))$ is a bounded function on the complementary of a negligible set. Consequently, $V(x^\circ(t), y^\circ(t))$ is an absolutely continuous function on $[0, +\infty)$ and the fundamental theorem of calculus holds. From relations (43) and (44) we thus obtain

$$\begin{aligned} J(u^\circ) &= \int_0^{+\infty} u^\circ(s) ds = \int_0^{t^\circ} u^\circ(s) ds \\ &\geq V(x^\circ(0), y^\circ(0)) - V(x^\circ(t^\circ), y^\circ(t^\circ)) \\ &= V(x_0, y_0), \end{aligned} \quad (46)$$

since $(x^\circ(t^\circ), y^\circ(t^\circ))$ belongs to $\mathcal{D}_{\bar{y}}^-$ and thus $V(x^\circ(t^\circ), y^\circ(t^\circ)) = 0$ by construction.

Consider now the solution of the candidate optimal control u^* and the associated solution $(x^*(t), y^*(t))$ with initial condition (x_0, y_0) . From Proposition 3(i), we know that the solution belongs to $\mathcal{D}_{\bar{y}}^+$ for t in $[T_0, T_1]$. For t in $[T_0, T_1]$, we have the following chain of equalities:

$$\begin{aligned} \dot{V}(x^*(t), y^*(t)) &= V_x(x^*, y^*)\dot{x}^* + V_y(x^*, y^*)\dot{y}^* \\ &= V_x(x^*, \bar{y})\dot{x}^* \\ &= -\rho(x^*, \bar{y})V_y(x^*, \bar{y})\gamma\bar{y} \\ &= -u^*(t), \end{aligned} \quad (47)$$

where the second equivalence follows from Proposition 3(i) and from (33), the third one from Proposition 3(i), (36) and from the fact that $h(x^*(t), y^*(t)) = x^*(t)$ whenever $y^*(t) = \bar{y}$ (cf. Lemma 4(ii)), and the last one from Lemma 6(iv) and from (32). Thanks to the fact that $(x^*(T_0), y^*(T_0)) \in \mathcal{D}_{\bar{y}}^+$, $(x^*(T_1), y^*(T_1)) \in \mathcal{D}_{\bar{y}}^-$ and (47), this yields

$$\begin{aligned} J(u^*) &= \int_0^{+\infty} u^*(s) ds = \int_{T_0}^{T_1} u^*(s) ds \\ &= V(x^*(T_0), y^*(T_0)) - V(x^*(T_1), y^*(T_1)) \\ &= V(x^*(T_0), y^*(T_0)) \\ &= V(x_0, y_0) \\ &\geq J(u^\circ), \end{aligned} \quad (48)$$

where the last equality follows from Remark 7 and the last inequality from (46). Finally, relations (40) and (48) imply

$$J(u) \geq J(u^\circ) \geq J(u^*).$$

As u was chosen to be any feasible control function, this proves the optimality of u^* . Since u^* is feasible by Proposition 3(iii), the proof of existence in Theorem 1 is now completed.

We now prove uniqueness. Suppose u in $\mathcal{U}_{x_0, y_0}^{\bar{y}}$ is optimal. Following previous considerations, similarly defining t° as the first time the corresponding solution (x^u, y^u) exits the region $\mathcal{D}_{\bar{y}}^+$ and defining u° as in (39), we notice that inequality (40) must now be an equality. This forces $u(t) = 0$ for $t > t^\circ$. We now consider $u(t)$ for $t \leq t^\circ$ and we prove that u must be 0 before the solution reaches the threshold value \bar{y} . We define $\mathcal{C} = \{t \in [0, t^\circ] \mid y^u(t) < \bar{y}, u(t) > 0\}$ and prove that, indicating with μ the Lebesgue measure, $\mu(\mathcal{C}) = 0$. Suppose by contradiction that instead $\mu(\mathcal{C}) > 0$. Then standard considerations on the Lebesgue integral imply that

$$\int_{\mathcal{C}} u(s) ds > \int_{\mathcal{C}} \frac{y^u(s)}{\bar{y}} u^\circ(s) ds.$$

Combining this with the second inequality in (43) and following steps as in (46), we obtain

$$\int_0^{t^\circ} u(s) ds > \int_0^{t^\circ} \frac{y^u(s)}{\bar{y}} u^\circ(s) ds \geq V(x_0, y_0). \quad (49)$$

This contradicts the supposed optimality of u and implies that $\mu(\mathcal{C}) = 0$. Since u is assumed to be right-continuous and y is continuous, this implies that $u(t) = 0$ for every t such that $y^u(t) < \bar{y}$. In conclusion, u has to be null as long as the second component $y^u(t)$ of the solution stays below the threshold value \bar{y} and from the first time the solution exits $\mathcal{D}_{\bar{y}}^+$. Therefore, it can only be non null when the solution is such that $y^u(t) = \bar{y}$ and $x^u(t) > \bar{x}$. We now conclude by showing that, necessarily $u(t) = \rho(x^u(t), \bar{y})$ in all such points. We first notice that we must have $u(t) \geq \rho(x^u(t), \bar{y})$. Indeed, if $u(\bar{t}) < \rho(x^u(\bar{t}), \bar{y})$ for some \bar{t} , equations 4 and the right-continuity of u imply that u would not be feasible as it would allow the component y^u to exceed \bar{y} in a right neighborhood of \bar{t} . Moreover, if $u(\bar{t}) > \rho(x^u(\bar{t}), \bar{y})$ at some point \bar{t} , then, similarly, y^u would be decreasing in a right neighborhood of \bar{t} and thus u would be non null in instants where y^u is below

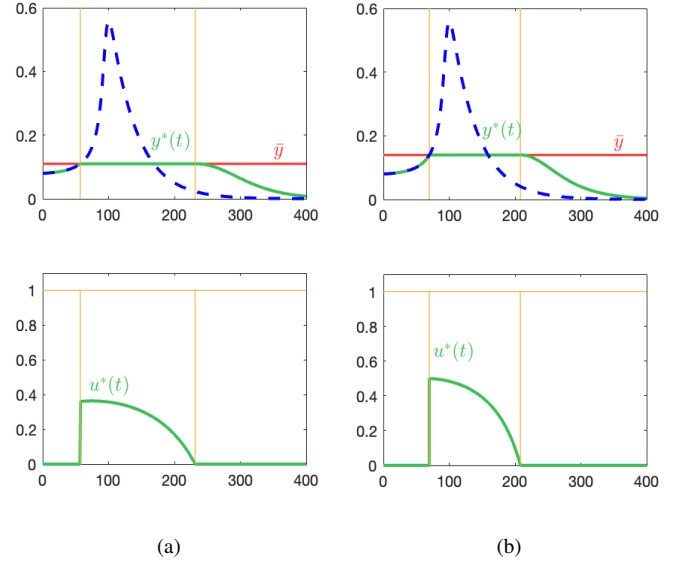


Fig. 3: Numerical counterexample illustrating the filling-the-box strategy for two different thresholds: (a) $\bar{y} = 0.11$ and (b) $\bar{y} = 0.154$. In each case, the top plot shows the infection dynamics: the uncontrolled epidemic is represented by the blue dashed curve, while the controlled trajectory under the filling-the-box strategy is plotted in green. The bottom plot reports the corresponding control function applied over time.

\bar{y} . As this fact was already shown to lead to non optimality, is also forbidden for u . This proves that $u(t) = \rho(x^u(t), \bar{y})$ the solution is such that $y^u(t) = \bar{y}$ and $x^u(t) > \bar{x}$, and thus is necessarily identical to u^* .

V. COUNTEREXAMPLE

In this section we provide a numerical counterexample that highlights the role of Assumption 1 in guaranteeing the optimality of the filling-the-box strategy. Specifically, we consider a transmission rate of the form $\beta(x, y) = (1 - 0.7x)y$, which does not satisfy Assumption 1 and under this setting, we show that the filling-the-box strategy is no longer optimal.

To illustrate this, we compare the cost of the filling-the-box strategy for two different thresholds \bar{y} . The initial condition is fixed at $y_0 = 0.08$ and $x_0 = 1 - y_0$. Figure 3 shows the two simulations. In each case, the top plot displays the evolution of the infection curve: the uncontrolled trajectory is represented by a blue dashed line, while the controlled trajectory obtained with the filling-the-box strategy is plotted in green. The bottom plot shows the corresponding control function applied over time.

When the threshold is set to $\bar{y} = 0.11$, the policy produces a total cost of 47.7. Surprisingly, increasing the threshold to $\bar{y} = 0.154$ leads to a higher total cost of 51.44. As the control signal implemented for $\bar{y} = 0.11$ is also feasible for $\bar{y} = 0.154$, this proves that the filling-the-box strategy is not optimal for this transmission rate. The explanation for this fact is that, since the reproduction number in this example is increasing in y , keeping the infection curve at

the highest admissible level allows to deactivate the control sooner, but requires a stronger intervention (as the bottom plots of Figure 3 illustrate), resulting in a larger cumulated cost. This example shows that when Assumption 1 is not satisfied, the simple filling-the-box strategy may fail to be optimal. In such situations, the timing of interventions becomes critical, and optimal policies may require more sophisticated strategies than a fixed-threshold rule.

VI. CONCLUSION

This paper has addressed the optimal control of a behavioral-feedback SIR epidemic model in which the infection rate depends in feedback on both the fraction of susceptible and infected agents. Under a general monotonicity condition on the feedback mechanism, the infection curve is proven to be unimodal as in the classical SIR model. Building on this property, we studied an optimal control problem that minimizes intervention costs while keeping the infection curve below a prescribed threshold over an infinite time horizon. Through a geometric analysis of the uncontrolled dynamics, we showed that, under mild regularity and monotonicity assumptions, the filling-the-box strategy is the unique optimal control, among the feasible right-continuous control signals.

Our work suggests several directions for future research. A first step would be to generalize the cost functional, for instance by introducing nonlinear intervention costs or by explicitly incorporating the social and economic burden of infections. Another natural extension is to consider delays in the infection rate, reflecting the realistic lag in observing and reacting to epidemic dynamics. Finally, extending the framework to structured populations or complex networks would provide further insights into the interplay between behavioral feedback and optimal control.

REFERENCES

- [1] M. Alutto, "Network effects and behavioral feedback in epidemic models," *PhD Thesis*, Politecnico di Torino - Università di Torino, 2025.
- [2] W. O. Kermack and A. G. McKendrick, "A contribution to the mathematical theory of epidemics," *Proceedings of the Royal Society of London. Series A*, vol. 115, no. 772, pp. 700–721, 1927.
- [3] H. W. Hethcote, "The mathematics of infectious diseases," *SIAM Review*, vol. 42, pp. 599–653, 2000.
- [4] A. G. McKendrick, "Applications of mathematics to medical problems," *Proceedings of the Edinburgh Mathematical Society*, vol. 44, pp. 98–130, 1925.
- [5] O. Diekmann and J. A. P. Heesterbeek, *Mathematical Epidemiology of Infectious Diseases: Model Building, Analysis and Interpretation*. Wiley, 2000.
- [6] A. W. Crosby, *America's Forgotten Pandemic: The Influenza of 1918*. Cambridge University Press, 2003.
- [7] J. T. Lau, X. Yang, E. Pang, H. Tsui, E. Wong, and Y. K. Wing, "SARS-related perceptions in Hong Kong," *Emerging infectious diseases*, vol. 11, no. 3, p. 417, 2005.
- [8] S. Hsiang, D. Allen, S. Annan-Phan, K. Bell, I. Bolliger, T. Chong, H. Druckenmiller, L. Y. Huang, A. Hultgren, E. Krasovich *et al.*, "The effect of large-scale anti-contagion policies on the COVID-19 pandemic," *Nature*, vol. 584, no. 7820, pp. 262–267, 2020.
- [9] W. H. Sandholm, *Population games and evolutionary dynamics*. MIT Press, 2010.
- [10] A. Satapathi, N. K. Dhar, A. R. Hota, and V. Srivastava, "Epidemic propagation under evolutionary behavioral dynamics: Stability and bifurcation analysis," in *American Control Conference (ACC)*. IEEE, 2022, pp. 3662–3667.
- [11] M. Ye, L. Zino, A. Rizzo, and M. Cao, "Game-theoretic modeling of collective decision making during epidemics," *Physical Review E*, vol. 104, no. 2, p. 024314, 2021.
- [12] K. Frieswijk, L. Zino, M. Ye, M. Cao, and A. Rizzo, "A mean-field analysis of a network behavioural-epidemic model," *IEEE Control Systems Letters*, vol. 6, pp. 2533–2538, 2022.
- [13] K. Paarom and C. Eksin, "SIS epidemics coupled with evolutionary social distancing dynamics," in *2023 American Control Conference (ACC)*. IEEE, 2023, pp. 2023–2028.
- [14] M. A. Amaral, M. M. Oliveira, and M. A. Javarone, "An epidemiological model with voluntary quarantine strategies governed by evolutionary game dynamics," *Chaos, Solitons & Fractals*, vol. 143, p. 110616, 2021.
- [15] K. A. Kabir and J. Tanimoto, "Evolutionary game theory modeling to represent the behavioural dynamics of economic shutdowns and shield immunity in the COVID-19 pandemic," *Royal Society Open Science*, vol. 7, no. 9, p. 201095, 2020.
- [16] N. C. Martins, J. Certório, and R. J. La, "Epidemic population games and evolutionary dynamics," *Automatica*, vol. 153, p. 111016, 2023.
- [17] J. Certório, N. C. Martins, and R. J. La, "Epidemic population games with nonnegligible disease death rate," *IEEE Control Systems Letters*, vol. 6, pp. 3229–3234, 2022.
- [18] S. Funk, M. Salathé, and V. A. Jansen, "Modelling the influence of human behaviour on the spread of infectious diseases: a review," *Journal of the Royal Society Interface*, vol. 7, no. 50, pp. 1247–1256, 2010.
- [19] F. Verelst, L. Willem, and P. Beutels, "Behavioural change models for infectious disease transmission: A systematic review (2010-2015)," *Journal of The Royal Society Interface*, vol. 13, 12 2016.
- [20] V. Capasso and G. Serio, "A generalization of the Kermack-McKendrick deterministic epidemic model," *Mathematical Biosciences*, vol. 42, no. 1, pp. 43–61, 1978.
- [21] R. Baker, "Reactive social distancing in a SIR model of epidemics such as COVID-19," *Physical Biology*, vol. 17, no. 4, 2020.
- [22] E. Franco, "A feedback SIR (fSIR) model highlights advantages and limitations of infection-dependent mitigation strategies," *arXiv preprint arXiv:2004.13216*, 2020.
- [23] A. Korobeinikov, "Lyapunov functions and global stability for SIR and SIRS epidemiological models with non-linear transmission," *Bulletin of Mathematical biology*, vol. 68, pp. 615–626, 2006.
- [24] M. Alutto, G. Como, and F. Fagnani, "On SIR epidemic models with feedback-controlled interactions and network effects," *2021 60th IEEE Conference on Decision and Control (CDC 2021)*, pp. 5562–5567, 2021.
- [25] M. M. Nguyen, "Upper bounds on overshoot in SIR models with nonlinear incidence," *npj Complexity*, vol. 1, no. 1, p. 11, 2024.
- [26] A. Srivastava, T. Das, and P. K. Srivastava, "Nonlinear dynamics of an SIRS model with ratio-dependent incidence and saturated treatment function," *Journal of Applied Mathematics and Computing*, vol. 70, no. 5, pp. 4537–4561, 2024.
- [27] Z. Feng and H. R. Thieme, "Endemic models with arbitrarily distributed periods of infection I: fundamental properties of the model," *SIAM Journal on Applied Mathematics*, vol. 61, no. 3, pp. 803–833, 2000.
- [28] W. Gao, Y. Wang, J. Cao, and Y. Liu, "Final epidemic size and critical times for susceptible-infectious-recovered models with a generalized contact rate," *Chaos: An Interdisciplinary Journal of Nonlinear Science*, vol. 34, no. 1, 2024.
- [29] W.-m. Liu, H. W. Hethcote, and S. A. Levin, "Dynamical behavior of epidemiological models with nonlinear incidence rates," *Journal of mathematical biology*, vol. 25, pp. 359–380, 1987.
- [30] S. Boatto, C. Bonnet, B. Cazelles, and F. Mazenc, "SIR model with time dependent infectivity parameter: approximating the epidemic attractor and the importance of the initial phase," CNRS, Working Paper hal-01677886, 2018, hAL Open Science, version 1. [Online]. Available: <https://hal.science/hal-01677886>
- [31] L. Zino and M. Cao, "Analysis, prediction, and control of epidemics: A survey from scalar to dynamic network models," *IEEE Circuits and Systems Magazine*, vol. 21, no. 4, pp. 4–23, 2021.
- [32] Y. Yi, L. Shan, P. E. Paré, and K. H. Johansson, "Edge deletion algorithms for minimizing spread in SIR epidemic models," *SIAM Journal on Control and Optimization*, vol. 60, no. 2, pp. S246–S273, Mar 2022.
- [33] R. Morton and K. H. Wickwire, "On the optimal control of a deterministic epidemic," *Advances in Applied Probability*, vol. 6, no. 4, pp. 622–635, 1974.
- [34] H. Behncke, "Optimal control of deterministic epidemics," *Optimal Control Applications and Methods*, vol. 21, no. 6, pp. 269–285, 2000.
- [35] F. Parino, L. Zino, and A. Rizzo, "Optimal control of endemic epidemic diseases with behavioral response," *IEEE Open Journal of Control Systems*, 2024.

- [36] T. Kruse and P. Strack, "Optimal control of an epidemic through social distancing," *SSRN Electronic Journal*, 2020.
- [37] L. Cianfanelli, F. Parise, D. Acemoglu, G. Como, and A. Ozdaglar, "Lockdown interventions in SIR models: Is the reproduction number the right control variable?" in *2021 60th IEEE Conference on Decision and Control (CDC)*. IEEE, 2021, pp. 4254–4259.
- [38] D. Acemoglu, V. Chernozhukov, I. Werning, and M. D. Whinston, "Optimal targeted lockdowns in a multigroup SIR model," *American Economic Review: Insights*, vol. 3, no. 4, pp. 487–502, 2021.
- [39] L. Miclo, D. Spiro, and J. Weibull, "Optimal epidemic suppression under an ICU constraint," *Journal of Mathematical Economics*, vol. 101, p. 102669, 2022.
- [40] D. Acemoglu, A. Fallah, A. Giometto, D. Huttenlocher, A. Ozdaglar, F. Parise, and S. Pattathil, "Optimal adaptive testing for epidemic control: combining molecular and serology tests," *Automatica : the journal of IFAC, the International Federation of Automatic Control*, vol. 160, 2024.
- [41] M. Alutto, L. Cianfanelli, G. Como, F. Fagnani, and F. Parise, "Behavioral-feedback SIR epidemic model: analysis and control," in *Proceedings of the 64th IEEE Conference on Decision and Control*, vol. <https://arxiv.org/abs/2509.12257>, 2025.
- [42] W. Rudin et al., *Principles of mathematical analysis*. McGraw-hill New York, 1976, vol. 3.
- [43] D. Liberzon, *Calculus of Variations and Optimal Control Theory: A Concise Introduction*. USA: Princeton University Press, 2011.
- [44] R. Kamalapurkar, P. Walters, J. A. Rosenfeld, and W. E. Dixon, *Reinforcement learning for optimal feedback control: A Lyapunov-based approach*, ser. Communications and Control Engineering. Springer International Publishing, 2018. [Online]. Available: <https://www.springer.com/us/book/9783319783833>
- [45] J. K. Hale, *Ordinary Differential Equations*, 2nd ed. Huntington, N.Y.: Robert E. Krieger Publishing Co., Inc., 1980.
- [46] A. Knauf, "Ordinary Differential Equations," in *Mathematical Physics: Classical Mechanics*, ser. UNITEXT. Berlin, Heidelberg: Springer, 2018, vol. 109.

APPENDIX

The right-hand side of (1) is locally Lipschitz with respect to (x, y, z) . Hence, on every time interval on which u is continuous, local existence and uniqueness of the solution for the corresponding Cauchy problem is a consequence of the Picard-Lindelöf theorem [45, I.3]). Consider now any interval \mathcal{I} admitting minimum t_0 on which u is continuous. By integrating equations in (1), assuming, for $t = t_0$, initial condition (x_0, y_0, z_0) in Δ , we get

$$x(t) = x_0 \exp \left(\int_{t_0}^t (-(1-u(\tau))\beta(x(\tau), y(\tau))y(\tau)) d\tau \right), \quad (50)$$

$$y(t) = y_0 \exp \left(\int_{t_0}^t ((1-u(\tau))\beta(x(\tau), y(\tau))x(\tau) - \gamma) d\tau \right), \quad (51)$$

$$z(t) = z_0 + \gamma \int_{t_0}^t y(\tau) d\tau. \quad (52)$$

Moreover, the sum of the equations in (1) gives $\dot{x}(t) + \dot{y}(t) + \dot{z}(t) = 0$. This implies that, as long as the solution $(x(t), y(t), z(t))$ exists, we must have that

$$x(t) \geq 0, y(t) \geq 0, z(t) \geq 0, \quad x(t) + y(t) + z(t) = 1. \quad (53)$$

In other terms, as long as the solution exists, it lives in Δ . In particular, this implies that the solution is globally defined on the whole of \mathcal{I} [46, Section 3.3]. We now construct a global solution on $[0, +\infty)$ in a recursive way. We order the discontinuity points as $t_1 < t_2 < \dots$. First, we let $u^k : [t_k, t_{k+1}] \rightarrow \mathbb{R}$ for $k \geq 0$ (letting $t_0 = 0$) to be the unique continuous function that coincides with u on $[t_k, t_{k+1}]$.

Similarly, we define $u^k : [t_k, +\infty) \rightarrow \mathbb{R}$ when the set of discontinuities is finite and has cardinality k . We now define $(x(t), y(t), z(t))$ on $[t_0, t_1]$ as the unique solution of the Cauchy problem relative to (1) with $u = u_0$ and initial condition (x_0, y_0, z_0) . Assuming the solution (x, y, z) to be constructed up to t_k with the desired properties, we extend it to the next discontinuity (or to $+\infty$ in case this was the last one) by considering the solution $(x^k(t), y^k(t), z^k(t))$ of the Cauchy problem on $[t_k, t_{k+1}]$ relative to the input function u_k and initial condition $(x(t_k), y(t_k), z(t_k))$. We then extend (x, y, z) to $[0, t_{k+1}]$ by setting $(x(t), y(t), z(t)) = (x^k(t), y^k(t), z^k(t))$ for $t \in [t_k, t_{k+1}]$. This construction yields the first part of the proposition.

Item (ii) is an immediate consequence of (51). The fact that $x(t)$ is non-decreasing follows from (53) and from the first equation in (1). The fact that it is strictly decreasing if and only if $x_0 > 0$ and $y_0 > 0$ follows from item (ii), which ensures that $y(t) > 0$ for every $t > 0$ if and only if $y_0 > 0$, and from (50), which ensures that $x(t) > 0$ if and only if $x_0 > 0$. This proves item (i).

To prove item (iii), note that point (x_e, y_e, z_e) in Δ is an equilibrium if and only if

$$\begin{cases} 0 = -(1-u)\beta(x_e, y_e)x_e y_e, \\ 0 = (1-u)\beta(x_e, y_e)x_e y_e - \gamma y_e, \\ 0 = \gamma y_e, \end{cases}$$

This implies that the points of the form $(x_e, 0, 1-x_e)$ are all equilibria and moreover, these are the only equilibria, since every point with $y_e \neq 0$ would not satisfy the equilibrium conditions given above. To prove item (iv), observe that the sum of the first two equations of (1) is $\dot{x}(t) + \dot{y}(t) = -\gamma y(t) \leq 0$. Since $x(t)$ and $x(t) + y(t)$ are decreasing functions, they both admit a limit:

$$x_\infty := \lim_{t \rightarrow +\infty} x(t), \quad \xi_\infty := \lim_{t \rightarrow +\infty} [x(t) + y(t)].$$

As a consequence, the following limit

$$y_\infty = \lim_{t \rightarrow +\infty} y(t) = \xi_\infty - x_\infty \geq 0 \quad (54)$$

exists. Suppose now by contradiction that $y_\infty > 0$. This means that there exist $T, M > 0$ such that $y(t) > M$, for all $t \geq T$. Then, we get

$$\begin{aligned} \lim_{t \rightarrow +\infty} [x(t) + y(t)] &= x(0) + y(0) - \gamma \int_0^\infty y(\tau) d\tau \\ &= x(0) + y(0) - \gamma \lim_{t \rightarrow +\infty} \int_0^t y(\tau) d\tau \\ &< x(0) + y(0) - \gamma \lim_{t \rightarrow +\infty} \int_T^t y(\tau) d\tau \\ &< x(0) + y(0) - \gamma M \lim_{t \rightarrow +\infty} (t - T) \\ &= -\infty \end{aligned}$$

As this is a contradiction, it must be $y_\infty = 0$. This concludes the proof.



Martina Alutto received the B.Sc. and the M.S. (cum laude) in Mathematical Engineering from Politecnico di Torino, Italy, in 2018 and 2021, respectively and the PhD in Pure and Applied Mathematics in 2025 at the Department of Mathematical Sciences, Politecnico di Torino, Italy. She was a Research Assistant at the National Research Council (CNR-IEIT), Torino, Italy. She is currently a Postdoctoral Researcher with the Royal Institute of Technology, Stockholm, Sweden. She was Visiting Student at Cornell University, Ithaca, NY in 2023. Her research interests focus on analysis and control of network systems, with application to epidemics and social networks.



Fabio Fagnani received the Laurea degree in Mathematics from the University of Pisa and the Scuola Normale Superiore, Pisa, Italy, in 1986. He received the PhD degree in Mathematics from the University of Groningen, Groningen, The Netherlands, in 1991. From 1991 to 1998, he was an Assistant Professor at the Scuola Normale Superiore. In 1997, he was a Visiting Professor at the Massachusetts Institute of Technology. Since 1998, he has been with the Politecnico di Torino. From 2006 to 2012, he acted as Coordinator of the PhD program in Mathematics for Engineering Sciences at Politecnico di Torino. From 2012 to 2019, he served as the Head of the Department of Mathematical Sciences, Politecnico di Torino. His current research focuses on network systems, inferential distributed algorithms, and opinion dynamics. He is an Associate Editor of the *IEEE Transactions on Automatic Control* and served in the same role for the *IEEE Transactions on Network Science and Engineering* and the *IEEE Transactions on Control of Network Systems*.



Leonardo Cianfanelli received the B.Sc. in Physics and Astrophysics in 2014 from Università di Firenze, Italy, the M.S. in Physics of Complex Systems in 2017 from Università di Torino, Italy, and the PhD in Pure and Applied Mathematics in 2022 from Politecnico di Torino, Italy. He is currently a Research Assistant at the Department of Mathematical Sciences, Politecnico di Torino, Italy. He was a Visiting Student at the Laboratory for Information and Decision Systems, Massachusetts Institute of Technology, in 2018–2020. His research focuses on control in network systems, with application to transportation and epidemics.



Giacomo Como is a Professor at the Department of Mathematical Sciences, Politecnico di Torino, Italy. He is also a Senior Lecturer at the Automatic Control Department, Lund University, Sweden. He received the B.Sc., M.S., and Ph.D. degrees in Applied Mathematics from Politecnico di Torino, Italy, in 2002, 2004, and 2008, respectively. He was a Visiting Assistant in Research at Yale University in 2006–2007 and a Postdoctoral Associate at the Laboratory for Information and Decision Systems, Massachusetts Institute of Technology in 2008–2011. Prof. Como currently serves as Senior Editor for the *IEEE Transactions on Control of Network Systems*, and as Associate Editor for *Automatica* and the *IEEE Transactions on Automatic Control*. He served as Associate Editor for the *IEEE Transactions on Network Science and Engineering* (2015–2021) and for the *IEEE Transactions on Control of Network Systems* (2016–2022). He was the IPC chair of the IFAC Workshop NecSys'15, a semiplenary speaker at the International Symposium MTNS'16, and the chair of the IEEE-CSS Technical Committee on Networks and Communications (2019–2024). He is recipient of the 2015 George S. Axelby Outstanding Paper Award. His research interests are in dynamics, information, and control in network systems.



Francesca Parise received the B.Sc. and M.Sc. (*summa cum laude*) degrees in information and automation engineering from the University of Padova, Padua, Italy, in 2010 and 2012, respectively, the graduate degree from the Galilean School of Excellence, University of Padova, in 2013, and the Ph.D. degree in information technology and electrical engineering from the Automatic Control Laboratory, ETH Zurich, Zurich, Switzerland, in 2016. She conducted her master's thesis research with Imperial College London, London, U.K., in 2012. From 2016 to 2020, she was a Postdoctoral Researcher with the Laboratory for Information and Decision Systems, MIT, and is currently an Assistant Professor of Electrical and Computer Engineering with Cornell University, Ithaca, NY. Her research interests include identification, analysis, and control of multiagent systems, with application to transportation, social, economic networks, and systems biology.